Adsorption of Methane and Hydrogen on Packed Beds of Activated Carbon

JOHN J. GESER and LAWRENCE N. CANJAR

Carnegie Institute of Technology, Pittsburgh, Pennsylvania

The adsorption of methane from mixtures of methane and hydrogen on fixed beds of activated carbon at —115°F. and 1 atm. has been studied. Inlet gas concentrations of 5.69, 7.58, and 10.65 mole % methane in hydrogen were employed over a gas flow rate range of from 3.24 to 16.3 std. cu. ft./hr. Activated carbon in sizes of 4 × 6 and 6 × 16 mesh and as 1/8- and 3/16-in. pellets were employed as adsorbent.

The external diffusion of adsorbate to the surface can be correlated by the usual mass transfer expressions for packed beds, although coefficients obtained in this work are lower than those reported for other systems in the literature.

A new equation is presented for internal particle diffusion.

This research was undertaken to determine the proper form of the rate equation which describes the adsorption of a component from a carrier gas on a fixed bed adsorbent. The systems which can be studied experimentally fall into two general classifications: those which produce wave fronts of constant shape and those whose wave fronts increase in length as they move through an adsorption bed. The system under consideration here consists of methane as the adsorbate; hydrogen, the carrier gas; and activated carbon, the adsorbent. It is of the constant wave front variety and exhibits a large heat effect.

THEORY

For the special case of constant wave front adsorption it can be shown that

$$q = \frac{q_\infty}{c_o} c \qquad (1)$$

or by defining new parameters one gets

$$y = x \qquad (2)$$

Also because of the constancy of shape of the wave front the usual partial differential equation which describes the material balance in an adsorber can be written in ordinary differential form. With these simplifications it can be shown that

$$\frac{dc}{d\theta} = k_g a_v \frac{\alpha c_o}{\rho_B q_\infty} (c - c^*) \qquad (3)$$

The rate equation which describes the resistance to mass transfer in the adsorbent particle is less clearly understood. It is dependent on diffusion within the pores of the particle and surface diffusion. These in turn are both complicated by the back diffusion of the carrier gas which originally saturated the adsorbent particle. In this paper a theoretical development of a rate equation based on such considerations will not be attempted. Instead it is postulated that the rate of internal mass transfer can be described by

$$\frac{dq}{d\theta} = K_p [(1 - x_{H_2}) q_\infty - q^*] \qquad (4)$$

Since this is not the usual mass transfer equation, the significance of the various terms should be noted. The term q in the left-hand side of the equation is determined from a material balance and related to the gas composition at the same point in the bed by Equation (1). q_∞ is the equilibrium value corresponding to c_o. x_{H_2} is a parameter which is zero for about 60 to 70% of the adsorption curve. It is obvious that x_{H_2} cannot be zero throughout the adsorption curve, because if it were the rate at the break point where q^* is zero would be given by

$$\frac{dq}{d\theta} = K_p q_\infty \qquad (5)$$

a nonzero value which is contrary to experimental observation. Therefore x_{H_2} must approach unity as q^* approaches zero.

If one divides Equation (3) by c_o and Equation (4) by q_∞ and notes Equation (2), the following equalities are obtained:

$$\frac{dy}{d\theta} = k_g a_v \frac{\alpha c_o}{P_B q_\infty} (y - y^*) = \frac{dx}{d\theta} = K_p [(1 - x_{H_2}) - x^*] \qquad (6)$$

For convenience the equilibrium data (*14, 16*) for this system are plotted in Figure 1 in terms of parameters x and y. Since q_∞ for all runs corresponds to a temperature of —115°F., only the —115-deg. isotherm has the coordinates (1,1) in Figure 1. For higher temperature isotherms the q^* or equilibrium value corresponding to c^* is less than q_∞ and gives a value of q^*/q_∞ less than unity. The diagonal of Figure 1 represents the material balance relationship given by Equation (1).

It should be noted that during adsorption q^* is always greater than q and c^* is always less than c. Therefore the equilibrium points which correspond to the interface conditions must always lie to the left of the diagonal.

EXPERIMENTAL APPARATUS

The apparatus consisted of a thermostated adsorption vessel, cylinders of prepurified hydrogen and prepared mixtures of methane and hydrogen, a multipoint-millivolt-recording system, and typical auxiliary equipment of piping and the like. The adsorption tubes were made of 1 in. I.D. welded 316 SS tubing with a 1/16-in. wall. The assembled adsorption vessel consisted of two main parts; and auxiliary-entrance-adsorption tube 15 in. long was connected to the base of the main adsorption vessel. The latter was made up of two 6-in. adsorption tubes connected by flanges to three measurement cells in such a manner that a measurement cell was located at the effluent end of each adsorption tube. The measurement cells consisted of disk-shaped pieces through which a 1-in. hole had been bored. A beveled metal-to-metal joint between the adsorption tubes and the measurement cells effected a low-temperature-gas-tight seal. The effluent concentrations were measured by way of the thermal-conductivity principle with bead thermistors located in bridge circuits. The thermal-conductivity cells consisted of a groove cut into the inner surface of the measurement cells in which the thermistors were located. Both the bed temperature and the temperature of the thermostat fluid, methylene chloride and dry ice, were measured with copper-constantan thermocouples. It was hoped that the adsorbent surface temperature could be measured by a thermocouple placed in the center of the absorbent bed so that it was in contact with and completely surrounded by the

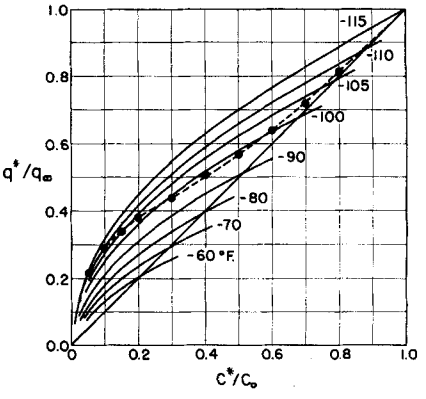

Fig. 1. Equilibrium isotherms, methane over activated carbon.

John J. Geser is with the California Research Corporation, Richmond, California.

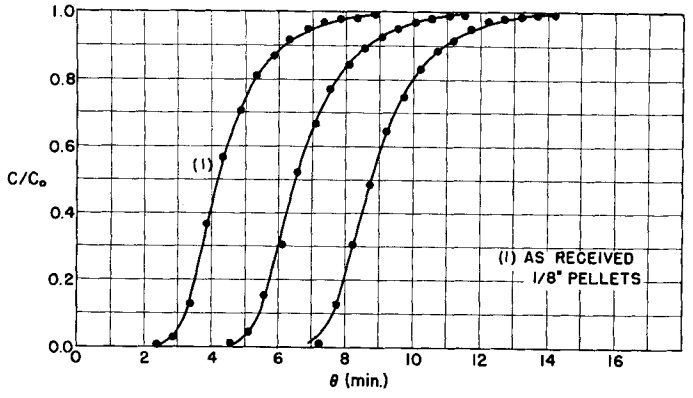

Fig. 2. C/C_o vs. time.

particles at the effluent end of each cell. This resulted in a time lag between the temperature wave and the concentration wave for which a correction had to be made. The emf signals from the thermal-conductivity bridges and the bed thermocouple were automatically recorded. The volumetric gas flow rate was determined by incremental timing of a calibrated wet-test meter. Pressure was determined at each measurement cell with calibrated inclined-mercury manometers. The gas was cooled to the thermostat temperature before entering the adsorption vessel in 40 ft. of one-quarter stainless steel tubing and before each measurement cell in 6-in. external coolers made of 3/16-in. stainless steel tubing.

Two types of activated carbon were used in this study: bone phosphate of lime type in sizes 4 × 6 and 6 × 16 mesh (U.S. sieve series) and sulfur × carbon type carbon as 1/8- and 3/16-in. cylindrical pellets. Both types were activated by heating in an oven at 225°F. for about 24 hr.

EXPERIMENTAL PROCEDURE

In order to conduct an adsorption run the bed was purged at room temperature with hydrogen which had been passed through a dry-ice trap. The vessel was then immersed in the thermostat and allowed to come to thermal equilibrium. A run was initiated by switching the gas feed from hydrogen to the desired mixture. After all the concentration curves had reached the inlet concentration level, the run was terminated by switching the gas feed back to hydrogen. After the methane desorbed, as indicated by the return of the thermal-conductivity-cell emf values to the hydrogen level, the gas flow was adjusted as desired and the subsequent run initiated. Multiple runs were made in this manner with no detectable effect on the adsorptive capacity of the bed.

Table 1 is a summary of the experimental conditions which were studied. Figure 2 illustrates the kind of data that is obtained by this technique. The first cell in the adsorption train was packed with adsorbent as received from the manufacturer; the next two cells contained screened material. The assumption of constant wave front is validated by these curves which are typical of all runs.

DATA ANALYSIS

There are two approaches to the problem of fitting Equation (4) to the experimental data. The slopes $dy/d\theta$, or their equivalent $dx/d\theta$, are calculated from curves like those illustrated on Figure 2. If one knows y and uses one of the usual external mass transfer correlations, such as that of Gamson (7), to calculate $k_g a_v$, a y^* may be estimated via Equation (6). From the temperature measurement and the equilibrium data plotted in Figure 1 a value of x^* is readily determined and the term K_g can be evaluated for zero values of x_{H_2}. Such an analysis however places all the uncertainty of the external mass transfer correlation into K_g.

Another approach is employed here. When one assumes that x_{H_2} is zero, sets of values for x^* and y^* are found by trial and error such that insertion of these values into Equation (6) gives constant values for $k_g a_v (\alpha c_o)/(\rho_B q_\infty)$ and K_g throughout the upper part of the adsorption curve. Sets of these x^*, y^* values are plotted on Figure 1 for one particular run. As expected K_g cannot be held constant throughout the adsorption curve for zero values of x_{H_2}. Therefore for the bottom 30% to 40% of the adsorption curve K_g is maintained constant by allowing x_{H_2} to vary. It can be seen in Figure 1 that when the x^*, y^* points have been determined in the upper region of the adsorption curve, the remainder of the curve can easily be drawn by eye. A summary of coefficients calculated from the experimental data is given in Table 1.

The proposed equation was first established by means of the 6 × 16 mesh particle size data.

Attempts to apply the same models to the data of the remaining particle sizes necessitated in some instances the assumption of a lower valued temperature profile than that measured. If the measured profile had been used in these cases, the surface-equilibrium curve (see Figure 1) would have fallen below the material-balance diagonal. Both the particle and the gas-phase

Table 1. Run Summary

Run no.	C_o, (mole %)	F, (std. cu. ft./hr.)	k_g, (ft./hr.)	K_g, (hr.$^{-1}$)	J_D	Bed data		
16	10.65	11.84	428	69.7	0.293	BPL 6 × 16 mesh	$W_1 = 0.1182$ (lb.)	$L_1 = 0.729$ (ft.)
17	10.65	6.99	360	69.7	0.418	$\rho_B = 29.83$ lb./cu. ft.	$W_2 = 0.0525$	$L_2 = 0.323$
19	7.58	7.10	335	69.7	0.385	$\alpha = 0.41$	$W_3 = 0.0510$	$L_3 = 0.323$
21	5.69	14.27	365	69.7	0.208	$\phi = 0.86$		
						$a_v = 264$ sq. ft./cu. ft.		
10	10.65	7.02	388	45.5	0.447	BPL 4 × 6 mesh	$W_1 = 0.1147$ (lb.)	$L_1 = 0.775$ (ft.)
11	10.65	14.09	419	45.5	0.241	$\rho_B = 26.56$	$W_2 = 0.0505$	$L_2 = 0.336$
12	7.58	13.58	395	45.5	0.233	$\alpha = 0.45$	$W_3 = 0.0504$	$L_3 = 0.328$
15	5.69	7.55	359	45.5	0.387	$\phi = 0.86$		
						$a_v = 131$ sq. ft./cu. ft.		
23	10.65	13.51	438	47.5	0.264	S × C 1/8-in. pellet	$W_1 = 0.1033$ (lb.)	$L_1 = 0.664$ (ft.)
25	7.58	6.90	318	47.5	0.375	$\rho_B = 29.10$	$W_2 = 0.0520$	$L_2 = 0.329$
29	5.69	14.14	441	47.5	0.253	$\alpha = 0.42$	$W_3 = 0.0504$	$L_3 = 0.315$
30	10.65	10.67	461	47.5	0.347	$\phi = 0.91$		
31	10.65	3.74	378	47.5	0.825	$a_v = 163$ sq. ft./cu. ft.		
33	10.65	3.24	245	34.6	0.611	S × C 3/16-in. pellet	$W_1 = 0.1005$ (lb.)	$L_1 = 0.708$ (ft.)
35	10.65	10.93	357	34.6	0.263	$\rho_B = 25.95$	$W_2 = 0.0467$	$L_2 = 0.346$
36	7.58	15.87	425	34.6	0.231	$\alpha = 0.48$	$W_3 = 0.0479$	$L_3 = 0.338$
38	5.69	8.11	393	34.6	0.390	$\phi = 0.91$		
40	10.65	16.13	413	34.6	0.205	$a_v = 94.3$		
41	10.65	5.90	307	34.6	0.419			

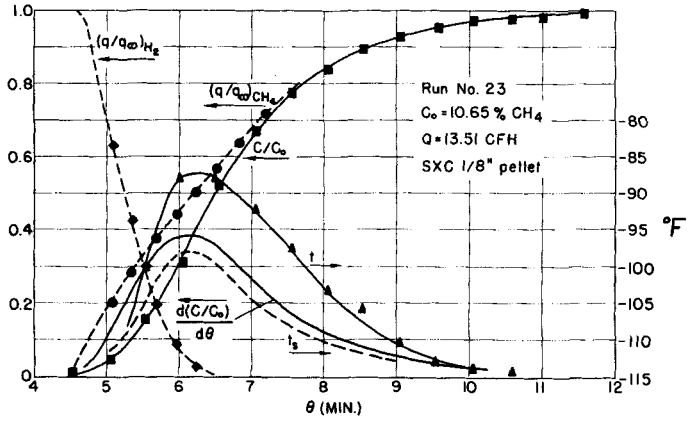

Fig. 3. Temperature and concentration profiles in adsorbent bed.

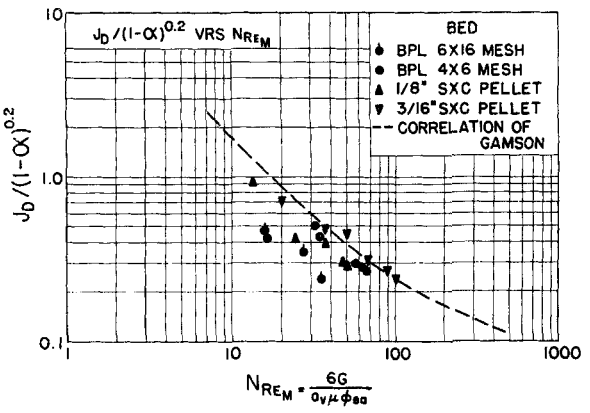

Fig. 4. External mass transfer correlation.

models would then predict negative adsorption rates. The worst case is shown in Figure 3 in which a correction of 10 deg. was made at the temperature-profile peak. 60% of the runs were fit to the models with no correction. The largest correction, 10°F., was made in two runs. The average correction based on the runs corrected (eight runs) was 8°F. Preliminary runs made with 12 × 20 mesh carbon indicated that the thermocouple could by chance be located in a hot spot, that is in a position where gas flow was restricted. Radiative and convective heat transfer from the bed could then raise the temperature of the thermocouple above the average surface temperature of the pellets. In future work it would be advisable not only to use very fine judiciously placed thermocouples, but also to use several connected in parallel to obtain a more representative average bed temperature.

The significance of the parameter x_{H_2} is a matter of speculation. The term q_∞ in Equation (4) is the ultimate capacity of the adsorbent under the conditions of the experimental run. Initially however the bed is saturated with hydrogen and the total capacity of such a bed is different from a bed in a vacuum. At low concentrations of methane, hydrogen is still competing for residence on the bed. The simplest relationship that may be written between the parameter x_{H_2} and the presence of hydrogen is

$$x_{H_2} = \left(\frac{q}{q_\infty}\right)_{H_2} \qquad (7)$$

There are two pieces of evidence, however weak, that support this hypothesis. First the form of x_{H_2}, plotted as $(q/q_\infty)_{H_2}$ on Figure 3, resembles that of a desorption curve, and it may well be the desorption curve for hydrogen. Secondly an experimental run was made in which, after the adsorption curve developed for a mixture of 3 mole % methane in hydrogen, pure methane was sent through the bed. The effluent curve indicated a step change, not the gradual desorption curve that might be expected if hydrogen were present in the bed. One is led to conclude therefore that above certain concentrations of methane in the gas phase hydrogen cannot reside in the bed. It is at these concentrations that x_{H_2} is zero. This hypothesis of course demands further experimental investigation.

OTHER MODELS

Before the rate equation given by Equation (4) was formulated the models suggested by other investigators were examined. Among these were the model presented by Klotz (*12*) which has been used by Drew, Spooner, and Douglas (*6*) and by Selke and Bliss (*15*); the model of Amundsen (2), of Glueckauf and Coates (9), and of Bohart and Adams (3). None of these could be applied to the data presented here.

DISCUSSION OF THE RESULTS

Gas-Phase Mass Transfer

If the transfer of material from the main-gas stream to the surface is correctly represented by Equation (6) and the interfacial concentrations have been correctly determined, one would expect the gas-phase mass transfer coefficients to correspond to the values obtained from existing generalized correlations. In accordance with Gamson (7), mass transfer coefficients for mass transfer in fixed beds may be correlated by the relationships

$$J_d = 1.46\left(\frac{6G}{a_v \mu \varphi_{ea}}\right)^{-0.41} (1-\alpha)^{0.2} \quad \text{for } \frac{6G}{a_v \mu \varphi_{ea}} > 100 \qquad (8)$$

and

$$J_d = 17\left(\frac{6G}{a_v \mu \varphi_{ea}}\right)^{-1.0} (1-\alpha)^{0.2} \quad \text{for } \frac{6G}{a_v \mu \varphi_{ea}} < 10 \qquad (9)$$

where by definition

$$J_d = \frac{k_g c_{fg} M_m}{G}\left(\frac{\mu}{P D_v}\right)_f^{2/3} \qquad (10)$$

The group

$$\frac{6G}{a_v \mu \varphi_{ea}} \qquad (11)$$

is a modified Reynolds number defined by Gamson. φ_{ea} is a correlation shape factor having a value 1 for spherical particles and a value less than 1 for nonspherical particles. It is that value which when incorporated into the modified Reynolds number and the right-hand side of the rate equation produces a J_d factor correlation which coincides with the spherical particle correlation. In order to make a direct graphical comparison with the correlation of Gamson J_d factors were calculated from mass transfer coefficients obtained here. Values of ϕ_{ea} and a_v must be determined to compare these mass transfer coefficients with those predicted by the Gamson correlation. ϕ_{ea} was assumed to be equal to 0.86 for the granular carbon (Gamson's flake value) and 0.91 for the cylindrical pellets as recommended by Gamson. As a first-order approximation the surface area per unit volume of packed bed values were determined by way of the Kozeny equation (*1, 4, 10, 15*) and the fixed-bed pressure-drop correlation of Chilton and Colburn (5). The external surface area per unit volume of bed is given by the expression

$$a_v = 2.54\left(\frac{A_x \Delta P \alpha^3}{Q L \mu}\right)^{1/2} \qquad (12)$$

When the modified Reynolds number is less than 40, the pressure drop across a bed of granular solids may be obtained from the equation

$$\Delta P = \frac{53 \mu L V_{op} A_f}{D_p^2} \qquad (13)$$

The wall-effect factor may be approximately related to the particle to tube diameter ratio by the linear relation

$$A_f \cong 1 - 1.5\frac{D_p}{D_t} \qquad (14)$$

After substitution of the latter two ex-

pressions Equation (12) becomes with cancellation of equivalent terms

$$A_v = 18.49\left[\frac{\left(1-1.5\frac{D_p}{D_t}\right)}{D_p^2}\alpha^3\right]^{1/2} \quad (15)$$

Since the particles are irregular in shape, the diameter of a sphere having an equivalent surface area per unit volume is used. Then

$$D_p = \frac{6\,(1-\alpha)}{A_v\,\phi} \quad (16)$$

It should be noted that ϕ and ϕ_{ea} are not strictly speaking the same quantity. ϕ is a geometrical quantity, the ϕ of Carman (*4*), while ϕ_{ea} is an empirical constant in the Gamson correlation. On the basis of values reported by Gamson and Carman for particles similar to those of this work there appears to be little difference in value. In analyzing the data consequently the values of ϕ were assumed equal to the ϕ_{ea} values of Gamson The binary diffusivity was determined by the correlation Equation (8)

$$D_v = 0.01664\,\frac{T^{3/2}}{P[v_A^{1/3}+v_B^{1/3}]^2}\sqrt{\frac{1}{M_A}+\frac{1}{M_B}} \quad (17)$$

The values of $J_d/(1-\alpha)^{0.2}$ based upon the k_g values obtained in this work are plotted in Figure 4 against the associated N_{Re} values. For purposes of comparison the correlation of Gamson is also plotted.

CONCLUSIONS

The adsorption of methane from mixtures of methane and hydrogen on activated carbon under the conditions of this work is of the controlled mass transfer fixed-wave-front type. The process cannot be considered isothermal, nor can the resistance to mass transfer be assigned alone to the gas phase or to the particle. A component for each must be considered. The models presented, although simplified and not the actual mechanism, appear to describe the data quite well. They have the proper limits and because of their simplicity are easy to appy. The agreement between the mass transfer coefficient correlation of Gamson is believed to support the assumed nature of the mechanism. The uncertainty in the bed temperature used to evaluate the surface-equilibrium-concentration values along with the uncertainty in the values of a_v for instance could easily account for the difference. Although the particle mechanism model appears to describe the data best, this is due in part to the method used in fitting the data. How the particle transfer coefficient varies with particle size, carbon type, and gas composition has not been determined.

ACKNOWLEDGMENT

This research was supported by a grant from the Petroleum Research Fund administered by the American Chemical Society. Grateful acknowledgment is hereby made to the donors of this fund.

NOTATION

A_f = wall effect factor in Equation (37)
A_r = cross-sectional area of column, sq.ft.
a_v = adsorbent bed mass transfer area per unit volume of bed, sq.ft./cu.ft.
c = gas phase concentration of methane at position Z and time t, lb. moles/cu.ft.
c_{fg} = mean value of the nontransferable component, lb. moles/cu.ft.
c_o = column inlet concentration of methane, lb. moles/cu.ft.
c^* = gas concentration in equilibrium with the adsorbate at the external surface of the adsorbent particle, lb. moles/cu.ft.
D_p = adsorbent particle diameter, ft.
D_t = diameter of adsorption tube, ft.
D_v = binary molecular gas diffusivity, ft./hr.
F = volumetric gas flow rate, std. cu.ft./hr.
G = mass flow rate, lb./hr. sq.ft.
J_d = mass transfer factor
k_g = gas-phase mass transfer coefficient, lb. moles/(hr.) (sq.ft.) (mole/cu.ft.)
K_p = particle mass transfer coefficient, hr.$^{-1}$
L = bed length, ft.
M_A = molecular weight of A
M_B = molecular weight of B
M_m = mean molecular weight of the gas film
P = total pressume, atm.
p = pressure drop across bed, lb./sq.ft.
q = concentration of methane on the adsorbent at position Z and time t, lb. moles/lb. of adsorbent
q^* = adsorbate concentration in equilibrium with the gas at the external surface of the particle, lb. moles/lb. of adsorbent
q_∞ = isotherm adsorbate concentration in equilibrium with c_o, lb. moles/lb. adsorbent
N_{Re_m} = modified Reynolds number defined by Equation (11), dimensionless
T = temperature, °K.
t_s = external surface temperature of adsorbent particle, °F.
v_a/v_b = molecular volumes of species A and B respectively
V_{sp} = superficial gas velocity, ft./hr.
W = weight of adsorbent bed of length L and diameter D_t
x = q/q_∞, dimensionless
x^* = q^*/q_∞, dimensionless
c = C/C_o, dimensionless
c^* = C^*/C_o, dimensionless
Z = distance from inlet of bed, ft.

Greek Letters

α = void fraction, cu.ft. voids/cu. ft. column
θ = time elapsed from the beginning of the adsorption process, hr.
μ = gas viscosity, lb./ft. hr.
ρ = gas density, lb./cu.ft.
ρ_B = bulk density of bed, lb. adsorbent/cu.ft. of column
ϕ = particle shape factor, dimensionless
ϕ_{ea} = correlation factor of Gamson, dimensionless

Subscript

f = evaluated at the temperature of the gas film

LITERATURE CITED

1. Allen, J. A., and C. J. Haigh, *J. Chem. Educ.*, **31**, 354 (1954).
2. Amundsen, N. R., *J. Phys. & Colloid Chem.*, **54**, 812 (1950).
3. Bohart, G. S., and E. Q. Adams, *J. Am. Chem. Soc.*, **42**, 523 (1920).
4. Carman, P. S., *J. Soc. Chem. Ind.*, **57**, 225 (1938); **58**, 1 (1939).
5. Chilton, T. H., and A. P. Colburn, *Trans. Am. Inst. Chem. Engrs.*, **26**, 178 (1931).
6. Drew, T. B., F. M. Spooner, and J. B. Douglas, cited in reference *13*.
7. Gamson, B. W., *Chem. Eng. Progr.*, **47**, 19 (1951).
8. Gilliland, E. R., *Ind. Eng. Chem.*, **26**, 681 (1934).
9. Glueckauf, E., and J. I. Coates, *J. Chem. Soc.*, **149**, 1315 (1947).
10. Gooden, E. L., and C. M. Smith, *Ind. Eng. Chem., Anal. Ed.*, **12**, 479 (1940).
11. Kasten, P. R., Leon Lapidus, and N. R. Amundsen, *J. Phys. Chem.*, **56**, 683 (1952).
12. Klotz, I. M., *Chem. Rev.*, **39**, 241 (1946).
13. Kozeny, J., *Ber. Wien Akak.*, **136a**, 271 (1927).
14. Pittsburgh Coke and Chemical Company, Private communication.
15. Selke, W. A., and Harding Bliss, *Chem. Eng. Progr.*, **46**, 509 (1950).
16. Titov, A., *Z. Physik. Chem.*, **74**, 641 (1910).

Manuscript received September 1, 1961; revision received February 19, 1961; paper accepted February 21, 1961. Paper presented at A.I.Ch.E. New York meeting.